Diagn Interv Radiol 2024; DOI: 10.4274/dir.2024.242714

PEDIATRIC RADIOLOGY

ORIGINAL ARTICLE

Imaging findings of primary lung tumors in children

H. Nursun Özcan[1]
Fırat Atak[2]
Berna Oğuz[1]
Tezer Kutluk[3]
Mithat Haliloğlu[1]

[1]Hacettepe University Faculty of Medicine, Department of Radiology, Division of Pediatric Radiology, Ankara, Türkiye

[2]Hacettepe University Faculty of Medicine, Department of Radiology, Ankara, Türkiye

[3]Hacettepe University Faculty of Medicine, Department of Pediatrics, Division of Pediatric Oncology, Ankara, Türkiye

PURPOSE

Pediatric lung tumors are primarily discussed in the surgical literature. However, limited research has been reported on their imaging findings, and only a few tumor types have been documented. Therefore, the aim of this article is to describe the imaging features of primary lung tumors in children.

METHODS

The archives of the pediatric radiology unit were reviewed for primary lung tumors documented between 2007 and 2023. In total, 24 patients (9 girls and 15 boys; aged 5 months to 16 years) were included in the study. Their demographic characteristics, clinical presentation, and histopathologic results were obtained. All imaging studies were reviewed by two radiologists for various findings (e.g., lymphadenopathy, atelectasis, pleural effusion, calcification, multiplicity, pneumothorax, axial and lobar location, laterality, tumor margin, mediastinal shift, contrast enhancement pattern, signal intensity on T1- and T2-weighted images, and diffusion pattern), and a final decision was made by consensus. The mean tumor size was compared between the benign and malignant groups using a t-test.

RESULTS

There were 15 (62.5%) benign tumors, as follows: inflammatory myofibroblastic tumor (IMT; n = 10, 41%), hemangioma (n = 2, 8%), pneumocytoma (n = 2, 8%), and mature cystic teratoma (n = 1, 4%). Moreover, there were 9 (37.5%) malignant tumors, as follows: pleuropulmonary blastoma (PPB; n = 6, 25%), adenocarcinoma (n = 2, 8%), and lymphoepithelioma-like carcinoma (LELC) (n = 1, 4%). The most frequently reported symptoms were cough, fever, dyspnea, chest pain, and recurrent infection; six patients reported no clinical symptoms. Fifteen tumors (62%) were located in the right lung. The mean tumor diameter at the time of diagnosis was 6.4 ± 3 cm (benign group: 6.7 ± 3.4 cm; malignant group: 6 ± 2.3 cm, $P > 0.050$). Calcification was present in 80% of the patients with IMT. At the time of diagnosis, two (8.3%) patients were found to have metastasis: one was diagnosed with adenocarcinoma and the other with LELC. Tumors were located peripherally in 18 (75%) patients.

CONCLUSION

The symptoms associated with lung masses are non-specific. There is no correlation between tumor size and malignancy. The most common tumors observed in this study were IMT and PPB, respectively. IMT is highly associated with calcification.

CLINICAL SIGNIFICANCE

Primary lung tumors are rarely seen in children, and they have different histopathological types. Calcification might be an important radiological clue for the diagnosis of IMT, which is the most common lung tumor in children.

KEYWORDS

Children, lung, cancer, CT, MRI, inflammatory myofibroblastic tumor

Corresponding author: H. Nursun Özcan

E-mail: drhnozcan@yahoo.com

Received 13 February 2024; revision requested 13 March 2024; last revision received 21 April 2024; accepted 21 May 2024.

Epub: 10.06.2024

Publication date: 06.11.2024

DOI: 10.4274/dir.2024.242714

You may cite this article as: Özcan HN, Atak F, Oğuz B, Kutluk T, Haliloğlu M. Imaging findings of primary lung tumors in children. *Diagn Interv Radiol.* 2024;30(6):419-426.

Primary lung tumors are uncommon in children, have a different histologic spectrum than adult lung tumors, and change with age.[1-3] Metastases and congenital lung masses constitute a substantial proportion of lung neoplasms in children. The incidence of primary, metastatic, and congenital/inflammatory lesions is reported to be 1:5:60.[4] The most prevalent metastatic tumors in the lungs are Wilms tumor and osteosarcoma.[5] Primary lung masses may be located in the tracheobronchial tree or parenchyma. Furthermore, parenchymal involvement may occur secondarily via local invasion of mediastinal or chest wall masses.

Patients typically present with non-specific and indistinct clinical symptoms. Delayed diagnosis is common due to the lack of specific symptoms and diverse imaging findings at presentation. The mortality rate for primary benign lung neoplasms in children is low (8.7%), and that for primary malignant tumors is approximately 30% overall.[6] It is paramount that radiologists have a comprehensive understanding of the histopathological spectrum of primary lung masses, enabling them to identify relevant imaging findings, make accurate differential diagnoses, and provide appropriate guidance, particularly considering the relatively low survival rates and often unremarkable clinical presentation.

Research on pediatric lung tumors is primarily found in surgical literature.[2,7] However, few studies have been conducted on the imaging findings of primary lung tumors in the pediatric population, and only a few tumor types have been reported.[1,8] The purpose of this paper is to report on our experience with primary lung tumors in children. We have reviewed our cases over the past 16 years and provided a detailed overview of their imaging findings with computed tomography (CT) and magnetic resonance imaging (MRI).

Main points

- Primary lung tumors in children are rare. Patients generally present with non-specific symptoms, and imaging features are highly variable.
- The majority of inflammatory myofibroblastic tumors are observed as well-defined, peripheral, and calcified masses.
- Persistent consolidation and atelectasis should alert the radiologist to neoplastic conditions.

Methods

The archive of the pediatric radiology unit was retrospectively reviewed for lung tumors documented between 2007 and 2023. The inclusion criteria were an available CT and/or MRI scan and pathologic diagnosis of a lung tumor. Tumors of metastatic and tracheobronchial origin were excluded. The search yielded 25 patients, 1 of whom did not have imaging studies available. Therefore, only the remaining 24 patients (9 girls and 15 boys; aged between 5 months and 16 years, median age: 7.5 years) were included in the study (Figure 1). The demographic features, imaging findings, and pathological results were documented. Informed consent was waived due to the retrospective nature of the data analysis. Approval was obtained from the Hacettepe University Non-Interventional Ethics Committee for this retrospective study (decision no: SBA 23/377; date: 30.11.2023).

Chest X-rays were evaluated for several potential findings, including the presence of pleural effusion, pneumothorax, focal abnormal opacity, and asymmetric density (radiolucency or radiopacity) of the hemithorax. No pleural effusion or pneumothorax was detected among the patients with available chest X-rays. Chest CTs and MRIs were assessed for the following characteristics: anatomic location of the tumor, tumor size, margins (smooth or lobulated), tumor pattern (cystic, solid, or mixed), contrast enhancement pattern (homogeneous or heterogeneous), presence of calcification, atelectasis, pleural effusion, pneumothorax, mediastinal shift, lymphadenopathy, local invasion, and metastasis at the time of diagnosis. A cystic component was considered present if septation or a fluid–fluid level was visible in any region within the mass, irrespective of the imaging study. Note that when an MRI scan is performed, regions with typical fluid intensity are classified as cystic. Furthermore, if post-gadolinium series were available, they were checked for contrast enhancement in these areas. In patients with only CT scans available, areas without marked contrast enhancement and densitometric measurements less than 20 HU were considered cystic. Contrast enhancement was determined by comparing the density of the solid component of the lesion with the muscle density in single-phase studies. It was considered positive if the densitometric value of the solid part was equal to or greater than the muscle density. In cases where at least a two-phase pre- and post-contrast image was obtained or two separate acquisitions were performed at different time points with and without contrast (if the acquisition parameters were the same), a change in tissue density greater than 20 HU was considered positive for contrast enhancement. The tumor size was determined via measuring the two greatest axial dimensions. In group analyses, the largest axial diameter was used. Pleural effusion or pneumothorax was considered positive if seen only on the ipsilateral side with the mass. Mediastinal lymph nodes were considered pathologic if the axial short axis diameter was larger than 7 mm.[9] Radiologic detection of local invasion can be challenging. Thus, in patients who underwent surgery, we checked whether local invasion was confirmed by the pathological findings. In cases where no pathology report was available, we used predefined imaging criteria for local invasion and deemed all suspicious cases as negative. For central tumors, local invasion was considered positive

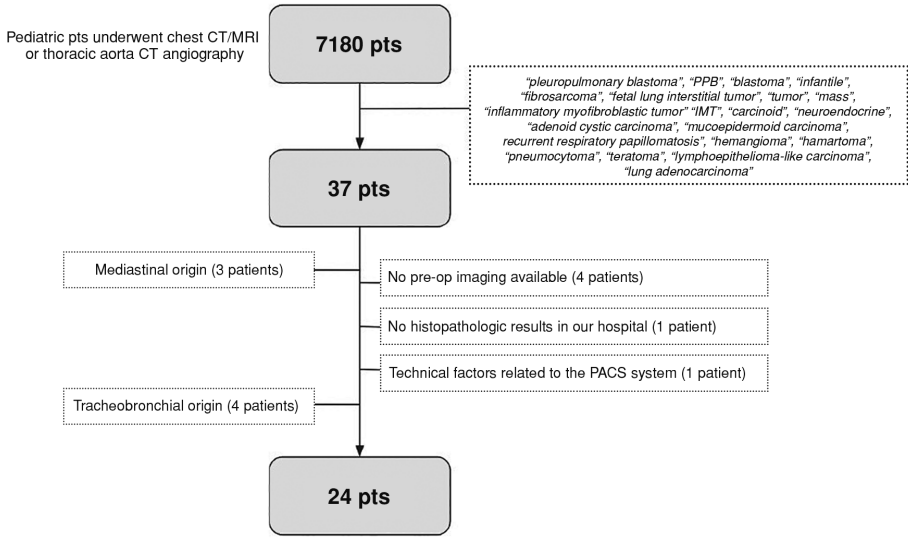

Figure 1. Flowchart of our study.

if, for example, there was an endobronchial nodular lesion, soft tissue density in the mediastinum showing continuity with the main lesion, intracardiac soft tissue lesion, or the presence of at least 180 degrees of surrounding hilar structures. In peripheral lesions, local invasion was considered positive if there was pleural thickening or nodularity, osseous destruction, and/or chest wall muscle involvement. If two radiologists could not reliably determine the presence of invasion, it was reported as negative. If the mass was located within the inner one-third of the concentric imaginary lines drawn from the hilum, it was considered central.[10] If the mass was within the borders of any two parts, the site that contained the majority of the tumor was reported as the tumor location.

Statistical analysis

The data were presented as the mean ± standard deviation or median (25^{th}–75^{th} percentile), as appropriate. Categorical variables were reported as the frequency (percentage). The normality assumption of the numerical variables was assessed with the Shapiro–Wilk goodness-of-fit test. Differences between groups were analyzed using the independent t-test, Mann–Whitney U test, or chi-squared (X^2) test. The statistical significance was set as $P < 0.050$.

Results

The patient demographics and clinical characteristics are summarized in Table 1. The chest X-ray and CT findings for the benign and malignant subgroups and the different histopathologic entities are presented in Tables 2 and 3. In total, 15 (62.5%) patients had benign neoplasms, comprising inflammatory myofibroblastic tumor (IMT; n = 10, 41.7%), hemangioma (n = 2, 8.3%), pneumocytoma (n = 2, 8.3%), and mature cystic teratoma (n = 1, 4.2%). The remaining 9 (37.5%) patients had malignant tumors, including pleuropulmonary blastoma (PPB; n = 6, 25%), adenocarcinoma (n = 2, 8.3%), and lymphoepithelioma-like carcinoma (LELC; n = 1, 4.2%). The most common presenting symptoms were cough (n = 12, 50%), fever (n = 7, 29.2%), dyspnea (n = 5, 20.8%), and chest pain (n = 5, 20.8%). There was no statistically significant difference in the demographics and clinical symptoms between the malignant and benign groups, except for regarding chest pain ($P = 0.03$; Table 4).

In total, 19 (79.2%) patients had available chest radiographs, 22 (91.7%) underwent CT scans, 2 (8.3%) underwent MRI scans, and 4 (16.7%) underwent both CT and MRI scans. Three (13.6%) CT examinations were performed without contrast material at other hospitals. The mass was found incidentally in six (25%) patients. Fifteen (62%) tumors were in the right lung and nine (37%) in the left lung. The frequencies of the involved lobes were as follows: right upper (n = 6, 25%), right lower (n = 6, 25%), left lower (n = 5, 20%), left upper (n = 4, 16%), and right middle (n = 3, 12%). The mean tumor size at the time of diagnosis was 6.4 ± 3 cm (6.7 ± 3.4 cm in the benign group and 6 ± 2.3 cm in the malignant group). The analysis revealed that there were no statistically significant differences in terms of tumor size between the malignant and benign groups ($P = 0.48$). Additionally, there was no statistically significant difference in the X-ray and CT findings between malignant and benign diseases, except for a higher prevalence of calcification in the benign tumors ($P = 0.01$).

Calcifications were present in eight patients with IMT (80%), one patient with PPB (16.6%), and one patient with mature cys-

Table 1. Demographics and clinical findings according to the benign and malignant subgroups

	Benign (n = 15)	Malign (n = 9)	Total (n = 24)	*P*
Demographics				
Age (y) (Median, 25p – 75p)	8 (11 months – 12)	4 (2.5 – 12)	7.5 (2 – 12)	0.92
Sex (F:M)	6:9	3:6	9:15	0.74
Clinical findings, n (%)				
Incidentally detected	4 (26.7%)	2 (22.2%)	6 (25%)	0.81
Cough	7 (46.7%)	5 (55.6%)	12 (50%)	0.67
Fever	4 (26.7%)	3 (33.3%)	7 (29.2%)	0.73
Recurrent infections	1 (6.7%)	0	1 (4.2%)	0.43
Neck swelling	0	1 (11.1%)	1 (4.2%)	0.19
Dyspnea	4 (26.7%)	1 (11.1%)	5 (20.8%)	0.36
Chest pain	1 (6.7%)	4 (44.4%)	5 (20.8%)	**0.03**
Dysphagia	1 (6.7%)	0	1 (4.2%)	0.43

Numbers in brackets are column percentages. F, female; M, male.

Table 2. Comparison of imaging features between the benign and malignant lesions

Imaging features	Benign (n = 15)	Malign (n = 9)	Total (n = 24)	*P*
X-ray*				
Abnormal opacity	9 (81.8%)	5 (62.5%)	14 (73.7%)	0.83
Asymmetrical lung opacity	1[α] (9.1%)	0	1 (5.3%)	0.70
CT				
Size (cm) (mean ± SD)	6.7 ± 3.4	6 ± 2.3	6.4 ± 3	0.48
Multiplicity	2 (13.3%)	1 (11.1%)	3 (12.5%)	0.87
Lobulated margin	9 (60%)	6 (66.6%)	15 (62.5%)	0.74
Contrast enhancement[β]				
Heterogeneous	5 (45.4%)	6 (75%)	11 (57.9%)	0.87
Homogeneous	6 (54.5%)	1 (12.5%)	7 (36.8%)	
Calcification	9 (60%)	1 (11.1%)	10 (41.7%)	**0.01**
Atelectasis	8 (53.3%)	7 (77.8%)	15 (62.5%)	0.23
Pleural effusion	8 (53.3%)	3 (33.3%)	11 (45.8%)	0.34
Local invasion	7 (46.6%)	3 (33.3%)	10 (41.7%)	0.52
Lymphadenopathy	4 (26.7%)	2 (22.2%)	6 (25%)	0.81
Metastasis	0	2 (22.2%)	2 (8.3%)	0.06

Numbers in brackets are column percentages. *No preoperative radiographs were available for four patients in the benign group and one patient in the malignant group. [α]An asymmetric radiolucent hemithorax was present on the contralateral side of the mass. [β]Two patients in the benign group and one patient in the malignant group did not have IV contrast studies. The mature cystic teratoma had a mildly enhancing solid nodule, and one pneumocytoma did not have apparent contrast enhancement. SD, standard deviation.

tic teratoma. The location of the tumor was peripheral in 18 patients (75%) and central in 6 patients (25%). Eleven tumors (57.9%) showed heterogeneous and seven (36.8%) homogeneous contrast enhancement. One (4.8%) pneumocytoma did not show any contrast enhancement, and the mature cystic teratoma presented with only a mildly enhancing solid nodular element. Notably, one adenocarcinoma (4.2%) and one LELC (4.2%) were found to be metastatic at the time of diagnosis.

Inflammatory myofibroblastic tumor

Ten children (four girls and six boys; mean age: 8.1 years) were diagnosed with IMT. Eight (8/10) tumors had calcification (Figure 2). The CT scans of two patients were performed without intravenous contrast. Five (62.5%) tumors showed heterogeneous enhancement, while three showed homogenous enhancement. Eight (80%) tumors were located peripherally, and seven (70%) were located at the lower zones. Six (60%) tumors had lobulated borders, while four (40%) had fine borders. Seven (70%) patients had pleural effusion, six (60%) had atelectasis, and four (40%) had lymphadenopathies. Moreover, seven patients (70%) had local invasion findings, with two showing pulmonary artery and vein invasion, two esophageal invasion, two pericardial invasion, and one left atrial invasion. No metastasis was detected. On MRI, both tumors were heterogeneous on T2- and T1-weighted images, hyperintense on T2-weighted images, and isointense/hyperintense on T1-weighted images. Both tumors showed heterogeneous contrast enhancement and diffusion restriction on MRI. Four of these tumors were previously reported.[5]

Hemangioma

Two (8.3%) children (a nine-month-old girl and a five-month-old boy) had hemangiomas. The CT scans revealed that both tumors were located peripherally, with lobulated margins and homogeneous contrast enhancement. The patient with giant hemangioma also demonstrated mediastinal shift. Due to the risk of bleeding, biopsy was not performed on either patient. Both patients were diagnosed as having hemangioma according to their radiologic findings, and they showed dramatic involution after propranolol treatment (Figure 3).

Pneumocytoma

Two (8.3%) children (a 13-year-old girl and a 15-year-old boy) had pneumocytoma. Both patients had single tumors. The tumors had different imaging features in the contrast-enhanced series, with one showing no apparent contrast enhancement and the other having homogeneous enhancement (Figure 4). One (50%) tumor was central. The two tumors had different margin characteristics: one was lobulated, and the other was smooth. The two CTs were unremarkable in terms of the other investigated parameters. However, ground-glass opacities resembling a "halo sign" were observed to surround one of the tumors. MRI was undertaken for only one patient and showed that the tumor was isointense to the paraspinal muscles on T1-weighted images and hyperintense on T2-weighted images. No restricted diffusion signal was observed on the diffusion-weighted imaging series.

Mature cystic teratoma

An 11-year-old boy was diagnosed with a mature cystic teratoma. The tumor had a maximum diameter of 15 cm and smooth margins and was located peripherally. It had a fluid density and calcification. Atelectasis and pleural effusion were also noted. A 1-cm mildly enhancing hyperdense nodule was detected within the tumor (Figure 5).

Pleuropulmonary blastoma

Six (25%) children (two girls and four boys; mean age: 3.3 years) were diagnosed with PPB. There were three (50%) type 2 tumors, two (33.3%) type 3 tumors, and one (16.7%) type 1 tumor. Calcification was found in only one (16.7%) patient. Five (100%) tumors (excluding a patient imaging performed without intravenous contrast) exhibited heterogeneous contrast enhancement. Four (66.6%) tumors had irregular margins. All six patients had atelectasis, three (50%) had pleural effusion, and one (16.7%) had pneumothorax. The MRI showed two (33.3%) tumors with solid and

Table 3. The imaging features of different histopathological entities

	IMT	PPB	Adenocarcinoma	Hemangioma	Pneumocytoma	MCT	LELC	Total
N of cases	10 (41.6%)	6 (25%)	2 (8.3%)	2 (8.3%)	2 (8.3%)	1 (4.2%)	1 (4.2%)	24
Age (y) (median, 25p – 75p)	8.5 (6 – 12)	3 (2 – 4)	9, 15*	5 mo, 9 mo*	13, 15*	11 mo*	16	7.5 (2 – 12)
L:R	4:6	3:3	0:2	1:1	1:1	0:1	0:1	9:15
Peripheral location	8 (80%)	6 (100%)	0	2 (100%)	1 (50%)	1 (100%)	0	18 (75%)
Greatest axial diameter (cm) (Median, 25p – 75p)	7.9 (5.5 – 10)	7.75 (6.8 – 9.2)	4, 4.4[α]	4, 8.2[α]	2.3, 2.4[α]	15	2.8	7.25 (4.25 – 9.6)
Calcification	8 (80%)	1 (16.7%)	0	0	0	1 (100%)	0	10 (41.6%)
Atelectasis	6 (60%)	6 (100%)	1 (50%)	1 (50%)	0	1	0	15 (62.5%)
Heterogeneous enhancement	5 (62.5%)[β]	5 (100%)[β]	1 (50%)	0[β]	0[b]	NE	NA	11 (57.9%)
Lobulated margin	6 (60%)	4 (66.6%)	2 (100%)	2 (100%)	1 (50%)	0	0	15 (62.5%)
Pleural effusion	7 (70%)	3 (50%)	0	0	0	1 (100%)	0	11 (45.8%)
Lymphadenopathy	4 (40%)	0	1 (50%)	0	0	0	1 (100%)	6 (25%)
Local invasion	7 (70%)	2 (33.3%)	1 (50%)	0	0	0	0	10 (41.6%)
Metastasis	0	0	1 (50%)	0	0	0	1 (100%)	1 (4.2%)

Numbers in brackets are column percentages. *Patients' ages are given separately. [α]Tumor sizes are given separately. [β]Two patients with IMT and one with PPB did not undergo preoperative CT or MRI with intravenous contrast. Homogeneous contrast enhancement was observed in two patients with hemangioma and one patient with pneumocytoma. IMT, inflammatory myofibroblastic tumor; PPB, pleuropulmonary blastoma; CT, computed tomography; MRI, magnetic resonance imaging; MCT, mature cystic teratoma; LELC, lymphoepithelioma-like carcinoma; NE, no enhancement; NA, not available; mo, months; L:R: left lung:right lung.

Table 4. A comprehensive presentation of individual tumor characteristics

Patient	Diagnosis	Age (yo)	Sex	Initial symptoms	Imaging studies	Location	Size (cm)	Contours	Contrast enhancement pattern	Calcification	Atelectasis	Peripheral	Pleural effusion	LAP	Local invasion	Metastasis
1	IMT	15	M	Cough, dyspnea, chest pain	CT	LLL	5.5×3.7	Lobulated	Heterogenous	+	+	-	+	-	+	-
2	IMT	8	M	Fever, cough, dyspnea	CT	RLL	11x8	Smooth	Homogeneous	+	+	+	+	+	+	-
3	IMT	9	M	Incidental	CT	RML	10×8	Lobulated	NA	+	-	+	+	+	+	-
4	IMT	12	M	Fever, cough	CT	RLL	7x6	Smooth	Heterogenous	+	+	+	+	-	-	-
5	IMT	2	F	Fever, recurring infection	CT	RUL	7.7×6.6	Lobulated	NA	+	+	+	-	-	+	-
6	IMT	12	F	Dysphagia	CT, MRI	LLL	10×6.5	Lobulated	Heterogenous	+	+	+	+	-	+	-
7	IMT	6	M	Incidental	MRI	LUL	6.6×8.1	Lobulated	Heterogenous	-	+	-	+	-	-	-
8	IMT	9 mo	F	Incidental	CT	LUL	4.1×3.6	Smooth	Homogenous	-	-	+	+	+	+	-
9	IMT	7	M	Cough	CT	RLL	5×4	Lobulated	Heterogenous	+	-	+	-	+	+	-
10	IMT	10	F	Cough	CT	RLL	10x8	Smooth	Homogenous	+	-	+	-	-	-	-
11	PPB	9	M	Cough, dyspnea, chest pain	CT	RLL	8×7.3	Smooth	Heterogenous	-	+	+	-	-	-	-
12	PPB	2	M	Incidental	CT	LUL	5×4.5	Lobulated	NA	-	+	+	-	-	-	-
13	PPB	4	M	Cough, fever, chest pain	CT, MRI	RML	6.3×7.5	Lobulated	Heterogenous	-	+	+	+	-	+	-
14	PPB	3	F	Cough, fever, chest pain	CT	RUL	6.8×6	Lobulated	Heterogenous	+	+	+	+	-	+	-
15	PPB	21 mo	F	Fever	MRI	LLL	10×8	Lobulated	Heterogenous	-	+	+	-	-	-	-
16	PPB	3	M	Chest pain	CT	LLL	9.2×8.7	Smooth	Heterogenous	-	+	+	+	-	-	-
17	Adenocarcinoma	15	F	Cough, neck swelling	CT	RML	4.4×3.8	Lobulated	Homogenous	-	+	-	-	+	+	+
18	Adenocarcinoma	9	M	Cough	CT, MRI	RUL	4×3.8	Lobulated	Heterogenous	-	-	-	-	-	-	-
19	Hemangioma	9 mo	F	Dyspnea	CT	LLL	8.2×7.5	Lobulated	Homogenous	-	+	+	-	-	-	-
20	Hemangioma	5 mo	M	Fever	CT	RUL	4×3	Lobulated	Homogenous	-	-	+	-	-	-	-
21	Pneumocytoma	15	M	Incidental	CT, MRI	RUL	2.3×1.7	Lobulated	Homogenous	-	-	+	-	-	-	-
22	Pneumocytoma	13	F	Cough	CT	LUL	2.4×2.3	Smooth	Absent	-	-	-	-	-	-	-
23	Mature cystic teratoma	11 mo	M	Cough, dyspnea	CT	RLL	15×15	Smooth	Absent	+	+	+	+	-	-	-
24	LELC	16	M	Incidental	CT	RUL	2.8×2.5	Smooth	NA	-	-	-	-	+	-	+

IMT, inflammatory myofibroblastic tumor; PPB, pleuropulmonary blastoma; MEC, mucoepidermoid carcinoma; LELC, lymphoepithelioma-like carcinoma; yo, years old; mo, months old; RUL, right upper lobe; RML, right middle lobe; RLL, right lower lobe; LUL, left upper lobe; LLL, left lower lobe; NA, not applicable; CT, computed tomography; MRI, magnetic resonance imaging; M, male; F, female; LAP, lymphadenopathy.

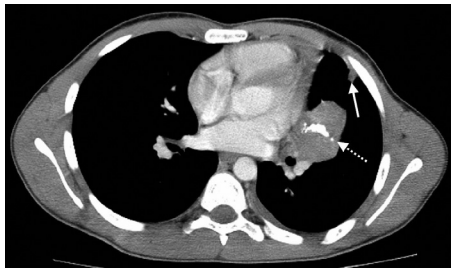

Figure 2. A 15-year-old boy with inflammatory myofibroblastic tumor. The axial contrast-enhanced computed tomography image shows a lobulated mass with heterogeneous enhancement and calcifications (dashed arrow) in the left upper lobe. Note the subpleural atelectasis (arrow).

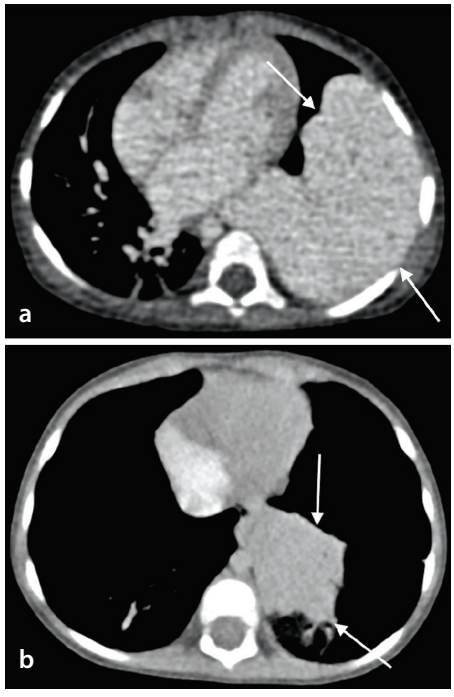

Figure 3. (a, b) A nine-month-old girl with hemangioma. **(a)** The axial contrast-enhanced computed tomography (CT) image shows large, homogenous contrast-enhanced tumor in the left lower lobe (arrows). **(b)** Following one year of propranolol treatment, a contrast-enhanced chest CT showed a significant decrease in the overall tumor size (arrows).

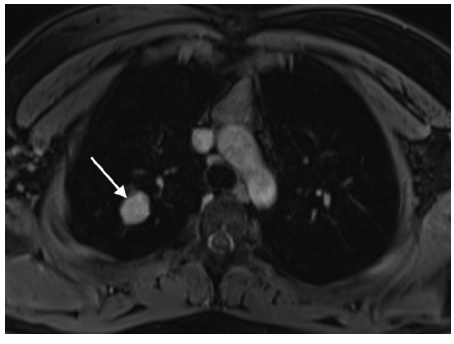

Figure 4. A 15-year-old girl with pneumocytoma. The axial contrast-enhanced T1-weighted image demonstrates a homogenously enhancing mass lesion (arrow).

cystic parts. The cystic parts were hyperintense on both T2- and T1-weighted images, indicating the presence of hemorrhage. The solid parts were heterogeneous due to cystic/necrotic areas and had lobulated margins. Both tumors had marked enhancement and diffusion restriction in the solid components (Figure 6). One type 2 tumor had local invasion into the mediastinum, and one type 3 tumor had right pulmonary vein thrombosis extending to the left atrium at the time of diagnosis. One patient with type 3 PPB developed brain metastasis during follow-up.

Adenocarcinoma

Two (8.3%) children (a 15-year-old girl and a 9-year-old boy) were diagnosed with adenocarcinoma. Both patients underwent CT, and one patient had both CT and MRI exams. One patient presented with bilateral and multifocal lesions along with interlobular septal thickening compatible with lymphatic spread. There were also visceral and lymph node metastases. The other patient had a central solitary tumor without atelectasis, lymphadenopathy, or local invasion. Neither tumor showed calcification. The tumor was hyperintense on T2-weighted images, isointense/hypointense on T1-weighted images, and had restricted diffusion signal (Figure 7).

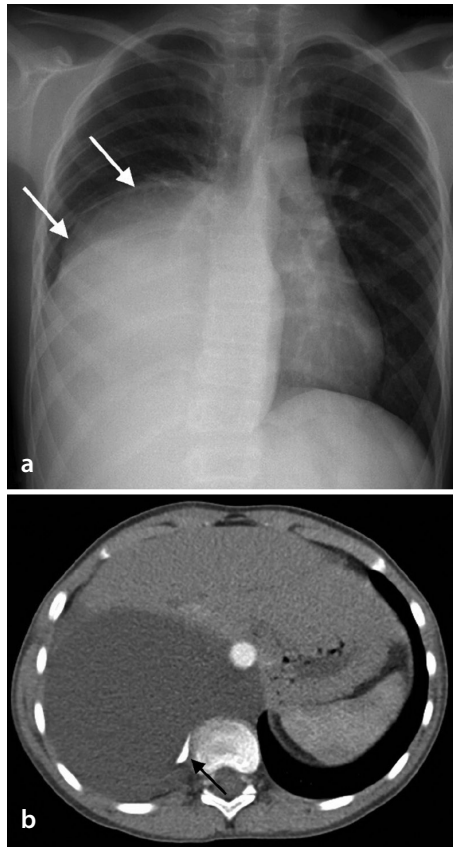

Figure 5. (a, b) An 11-month-old boy with mature cystic teratoma. **(a)** The chest X-ray shows large opacity in the lower zone of the right lung. **(b)** The axial chest computed tomography image demonstrates a large cystic mass with calcification (black arrow) and a nodular solid component (not shown).

Lymphoepithelioma-like carcinoma

A 16-year-old boy was diagnosed with LELC after a mass-like opacity was incidentally found on a chest X-ray in the right upper zone. The tumor measured 2.8 cm and was centrally located, with smooth margins and no calcification on CT. There was also mediastinal and ipsilateral hilar lymphadenopathy. It was not possible to comment on contrast enhancement due to the lack of pre-contrast

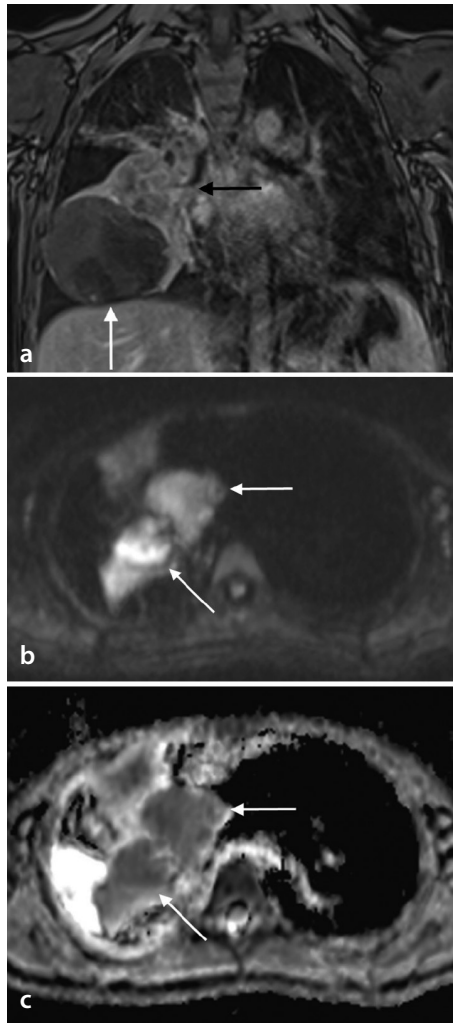

Figure 6. (a-c) A four-year-old boy with type 2 pleuropulmonary blastoma. **(a)** The coronal post-contrast magnetic resonance image shows a large and heterogeneous tumor with a lobulated margin consisting of solid (black arrow) and cystic (white arrow) parts. **(b)** The diffusion-weighted image (b = 800 s/mm2) and **(c)** apparent diffusion coefficient map show the diffusion restriction of the solid components of the tumor (arrows).

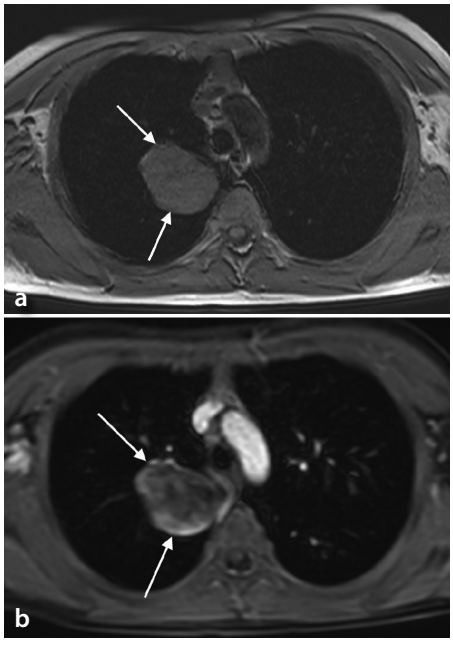

Figure 7. (**a, b**) A nine-year-old boy diagnosed with lung adenocarcinoma. **(a)** The axial T1- weighted image shows a well-circumscribed and isointense tumor in the right upper lobe (arrow). **(b)** Note the heterogenous enhancement on the T1-weighted post-contrast image (arrow).

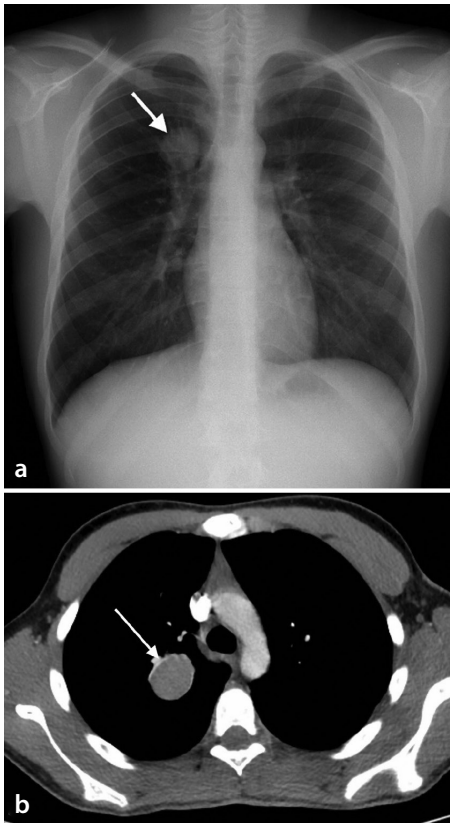

Figure 8. (**a, b**) A 16-year-old boy with lymphoepithelioma-like carcinoma. **(a)** The chest X-ray taken prior to the orthopedic surgery shows a nodule with smooth contours (arrow). **(b)** The axial contrast-enhanced chest computed tomography scan shows a uniform mass lesion (arrow).

images. There was neither pleural effusion nor atelectasis (Figure 8).

Discussion

This study yielded two major findings. First, pediatric patients with lung tumors generally have non-specific and indistinct clinical presentations, which can lead to misdiagnosis. Second, the most common lung tumors in children are benign, specifically dominated by IMT.

Previously known as inflammatory pseudotumor, plasma cell granuloma, or inflammatory fibrosarcoma, IMT is a rare mesenchymal tumor that may occur throughout the body, where the lung is the most affected organ.[11] The World Health Organization's fifth edition of Thoracic Tumors classifies IMT as having "borderline or uncertain behavior," possibly due to its potential for local invasion, tumor recurrence, and metastasis, despite previously being considered a benign entity.[12,13] Similar to the literature, in our series, the most common primary lung tumor was IMT.[2] However, in some patient cohorts, the most commonly reported tumor is carcinoid.[2,14] Among our patients, the most common presenting symptoms were cough and fever. IMT was predominantly located in the lower lung zones, consistent with the available literature.[12,15] Our study identified three major imaging findings suggestive of IMT, including calcification, peripheral location, and lobulated margins. In our series, calcification was present in four-fifths of the patients, whereas the literature reports varying rates (15%–77.8%) depending on the patient demographics and anatomic origins involved.[16,17] The inclusion of only parenchymal IMTs in our study may have contributed to this difference.[17] Additionally, calcification is reported to be more common in pediatric cases.[15,17] Atelectasis, pleural effusion, and local invasion were relatively common in our series, while lymphadenopathy was rare, which is consistent with the literature.[15]

Hemangioma, pneumocytoma, and mature cystic teratoma were the other benign tumors found in our patients. Pulmonary hemangioma is a rare tumor that typically presents as a solitary, well-defined lesion in the early neonatal period. Co-occurrence with other sites, such as the skin or liver, may be observed.[18] According to the classification system developed by the International Society for the Study of Vascular Anomalies, hemangiomas are categorized as either infantile or congenital based on the age of presentation and the presence of endothelial cell glucose transporter 1 (GLUT-1).[19] Infantile hemangiomas tend to grow after birth and are GLUT-1 positive. Dynamic CT and MRI studies may help to differentiate hemangiomas from other pulmonary tumors. Hemangiomas typically show early, peripheral and strong enhancement have sharply defined borders, and do not cause a mass effect.[20] Other presentations, such as multifocal masses, lesions with cystic spaces, and endobronchial lesions, may be seen.[1] Additionally, pulmonary artery or vein enlargement may be present due to increased supply.[1] Pneumocytoma (previously known as pulmonary sclerosing hemangioma) is a rare benign neoplasm of the lung and is frequently seen as a well-defined intraparenchymal nodular mass (often peripherally). Although size variability has been reported, most pneumocytomas are <3.5 cm in largest diameter,[21] which is compatible with our results. Although mediastinal teratomas are far from rare, primary pulmonary teratomas are extremely uncommon. Pulmonary teratomas present as encapsulated masses with a thin wall containing liquid tissue, fat, calcifications, or any such combination. In our single patient, the tumor was cystic with a mildly enhancing mural nodule and had calcified components.

PPB is the most common malignant primary lung tumor in the pediatric age group. Most patients are younger than six years old. Likewise, in our series, all patients except one (a nine-year-old boy) were under six years of age at the time of diagnosis.[1] PPB has three histopathological subtypes: type 1 is purely cystic (mean age: 10 months), type 2 is cystic and solid (mean age: 34 months), and type 3 is purely solid (mean age: 44 months).[1] Of note, the age at initial diagnosis is known to correlate with the subtype. In our series, there were three patients with type 2, two patients with type 3, and one patient with type 1. PPB has an association with *DICER1* gene mutations, and approximately 65%–70% of children with PPB display heterogeneous mutations.[22] Other tumors associated with *DICER1* mutations include cystic nephroma, pineoblastoma, pituitary blastoma, differentiated thyroid cancer, ovarian sex cord–stromal tumor, and embryonal rhabdomyosarcoma.[23-25] In the current study, due to the fact that these mutations have only been evaluated in very recent literature, our patients unfortunately did not undergo pertinent analyses. While most PPB cases are reported in the right hemithorax, in our series, three patients had left-sided lesions. At CT and MRI, type 1 tumors might appear as single or multicystic lesions. Type 2 tumors have air- or fluid-filled cavities with possible air–fluid levels along with solid internal nodules. Type

3 tumors are solid lesions. Pleural effusion and pneumothorax are frequently associated findings in PPB. In our series, three patients had pleural effusion, and only one had pneumothorax. One of our type 3 patients had right pulmonary vein thrombosis extending to the left atrium at the time of diagnosis, which is a rare but significant complication of PPB.

Adenocarcinoma is the most common subtype of non-small-cell lung cancer and is extremely rare in children and adolescents. Primary lung adenocarcinoma of children has the poorest prognosis, with a high prevalence of distant metastases.[26] Imaging findings are associated with histopathological classification and vary from a focal ground-glass nodule to a solid nodule or a mass.[26] They may present as mass-like consolidations and mimic pneumonia.

LELC is a large-cell carcinoma with prominent lymphocyte infiltration and is mostly seen in the nasopharynx. Similar to nasopharyngeal tumor, primary pulmonary LELC has a documented strong relationship with Epstein–Barr virus infection in Asian populations.[27] It usually presents with solitary pulmonary nodule or mass. However, primary pulmonary LELC in the pediatric population is extremely rare. During his preoperative workup for an orthopedic surgery, our patient was diagnosed with a chest X-ray incidentally. A subsequent chest CT was performed to confirm the presumptive diagnosis of a benign lesion, such as a bronchogenic cyst. Thus, it is important to note that small size or smooth appearance of a lesion does not exclude a malignant tumor.

Our study had some limitations. First, due to the retrospective design, the imaging studies were heterogenous. Second, we reviewed only the radiology archives of our institute and could therefore enroll a relatively small sample.

In conclusion, primary lung tumors are rarely seen in children, and they have different histopathological types. Patients generally have non-specific and indistinct clinical presentations, possibly delaying the initial diagnosis. It is noteworthy that calcification might be an important radiological clue for the diagnosis of IMT. Moreover, PPB is the most common malignant lung tumor in the pediatric age group and displays a wide range of imaging findings. Persistent consolidation and atelectasis should necessarily alert the radiologist regarding malignancy. Lastly, small size or smooth contouring of a lesion does not rule out a malignant tumor.

Conflict of interest disclosure

The authors declared no conflicts of interest.

References

1. Lichtenberger JP 3rd, Biko DM, Carter BW, Pavio MA, Huppmann AR, Chung EM. Primary lung tumors in children: Radiologic-pathologic correlation. *Radiographics*. 2018;38(7):2151-2172. [Crossref]
2. Yu DC, Grabowski MJ, Kozakewich HP, et al. Primary lung tumors in children and adolescents: a 90-year experience. *J Pediatr Surg*. 2010;45(6):1090-1095. [Crossref]
3. Giuseppucci C, Reusmann A, Giubergia V, et al. Primary lung tumors in children: 24 years of experience at a referral center. *Pediatr Surg Int*. 2016;32(5):451-457. [Crossref]
4. Cohen MC, Kaschula ROC. Primary pulmonary tumors in childhood: a review of 31 years' experience and the literature. *Pediatr Pulmonol*. 1992;14(4):222-232. [Crossref]
5. Eggli KD, Newman B. Nodules, masses, and pseudomasses in the pediatric lung. *Radiol Clin North Am*. 1993;31(3):651-666. [Crossref]
6. Hancock BJ, Di Lorenzo M, Youssef S, Yazbeck S, Marcotte JE, Collin PP. Childhood primary pulmonary neoplasms. *J Pediatr Surg*. 1993;28(9):1133-1136. [Crossref]
7. Rojas Y, Shi YX, Zhang W, et al. Primary malignant pulmonary tumors in children: a review of the national cancer data base. *J Pediatr Surg*. 2015;50(6):1004-1008. [Crossref]
8. Amini B, Huang SY, Tsai J, Benveniste MF, Robledo HH, Lee EY. Primary lung and large airway neoplasms in children: current imaging evaluation with multidetector computed tomography. *Radiol Clin North Am*. 2013;51(4):637-657. [Crossref]
9. Alves GR, Marchiori E, Irion KL, et al. Mediastinal lymph nodes and pulmonary nodules in children: MDCT findings in a cohort of healthy subjects. *American Journal of Roentgenology*. 2015;204(1):35-37. [Crossref]
10. Casal RF, Vial MR, Miller R, et al. What exactly is a centrally located lung tumor? Results of an online survey. *Ann Am Thorac Soc*. 2017;14(1):118-123. [Crossref]
11. Oguz B, Ozcan HN, Omay B, Ozgen B, Haliloglu M. Imaging of childhood inflammatory myofibroblastic tumor. *Pediatr Radiol*. 2015;45(11)1672-1681. [Crossref]
12. Narla LD, Newman B, Spottswood SS, Narla S, Kolli R. Inflammatory pseudotumor. *Radiographics*. 2003;23(3):719-729. [Crossref]
13. WHO Classification of Tumours Editorial Board, ed. Thoracic Tumours. In: WHO Classification of Tumours. Vol 5. 5th ed. ; 2021:288-290. [Crossref]
14. Shao W, Liu J, Li B, et al. Primary lung cancer in children and adolescents: analysis of a surveillance, epidemiology, and end results database. *Front Oncol*. 2023;13:1053248. [Crossref]
15. Agrons GA, Rosado-de-Christenson ML, Kirejczyk WM, Conran RM, Stocker JT. Pulmonary inflammatory pseudotumor: Radiologic features. *Radiology*. 1998;206(2):511-518. [Crossref]
16. Kim TS, Han J, Kim GY, Lee KS, Kim H, Kim J. Pulmonary inflammatory pseudotumor (inflammatory myofibroblastic tumor): CT features with pathologic correlation. *J Comput Assist Tomogr*. 2005;29(5):633-639. [Crossref]
17. Irodi A, Chacko BR, Prajapati A, et al. Inflammatory myofibroblastic tumours of the thorax: radiologic and clinicopathological correlation. *Indian J Radiol Imaging*. 2020;30(3):266-272. [Crossref]
18. Wheeler A, Kozakewich HP, Shashi K, Eng W. Pulmonary infantile hemangioma: clinical and histopathological review of eight cases. *Blood*. 2021;138(Suppl 1):4209-4209. [Crossref]
19. International Society for the Study of Vascular Anomalies. ISSVA Classification of Vascular Anomalies. issva.org/classification. [Crossref]
20. Pandya R, Tummala V. Giant infantile pulmonary hemangioma. *Pediatr Radiol*. 2010;40(Suppl 1):63-67. [Crossref]
21. Shin SY, Kim MY, Oh SY, et al. Pulmonary sclerosing pneumocytoma of the lung: CT characteristics in a large series of a tertiary referral center. Medicine (Baltimore). 2015;94(4):e498. [Crossref]
22. Dehner LP, Messinger YH, Schultz KAP, et al. Pleuropulmonary blastoma: evolution of an entity as an entry into a familial tumor predisposition syndrome. *Pediatr Dev Pathol*. 2015;18(6):504-511. [Crossref]
23. Bueno MT, Martínez-Ríos C, la Puente Gregorio A, et al. Pediatric imaging in DICER1 syndrome. *Pediatr Radiol*. 2017;47(10):1292-1301. [Crossref]
24. van Engelen K, Villani A, Wasserman JD, et al. DICER1 syndrome: approach to testing and management at a large pediatric tertiary care center. *Pediatr Blood Cancer*. 2018;65(1). [Crossref]
25. Sabapathy DG, Paul Guillerman R, Orth RC, et al. Radiographic screening of infants and young children with genetic predisposition for rare malignancies: DICER1 mutations and pleuropulmonary blastoma. *AJR Am J Roentgenol*. 2015;204(4):475-482. [Crossref]
26. Kayton ML, He M, Zakowski MF, et al. Primary lung adenocarcinomas in children and adolescents treated for pediatric malignancies. *J Thorac Oncol*. 2010;5(11):1764-1771. [Crossref]
27. Hoxworth JM, Hanks DK, Araoz PA, et al. Lymphoepithelioma-like carcinoma of the lung: radiologic features of an uncommon primary pulmonary neoplasm. *AJR Am J Roentgenol*. 2006;186(5):1294-1299. [Crossref]